

# A novel method for synthesis of nano- $\gamma$ - $\text{Al}_2\text{O}_3$ : study of adsorption behavior of chromium, nickel, cadmium and lead ions

A. Shokati Poursani · A. Nilchi · A. H. Hassani ·  
M. Shariat · J. Nouri

Received: 30 April 2014/Revised: 5 November 2014/Accepted: 22 December 2014/Published online: 14 January 2015  
© Islamic Azad University (IAU) 2015

**Abstract** Nano- $\gamma$ - $\text{Al}_2\text{O}_3$  adsorbent was synthesized by the novel sol–gel method. The adsorbent was characterized by transmission electron microscope, Fourier transform infrared and X-ray powder diffraction. The effects of several variables such as, adsorbent weight, pH and contact time on adsorption of chromium ( $\text{Cr}^{6+}$ ), nickel ( $\text{Ni}^{2+}$ ), cadmium ( $\text{Cd}^{2+}$ ) and lead ( $\text{Pb}^{2+}$ ) ions were studied in batch experiments. The results showed that the synthesized nano- $\gamma$ - $\text{Al}_2\text{O}_3$  had a good capacity to adsorb Cr and Pb. The kinetic data were described with pseudo-first- and pseudo-second-order models. Three isotherm models, namely Freundlich, Langmuir and Tempkin, were used for analysis of equilibrium data, and results showed that Langmuir and Freundlich models were suitable for describing the equilibrium data of  $\text{Cr}^{6+}$ ,  $\text{Cd}^{2+}$ ,  $\text{Ni}^{2+}$  and  $\text{Pb}^{2+}$ . Using Langmuir isotherm, the maximum sorption capacities of  $\text{Cr}^{6+}$ ,  $\text{Pb}^{2+}$ ,  $\text{Cd}^{2+}$  and  $\text{Ni}^{2+}$  were estimated to be 13.3, 6, 1.1 and 0.33 (mg/g) at 25 °C, respectively. The sorption capacity did not change remarkably after reuse of sorbent for sorption–desorption cycle. The selectivity order of  $\text{Cr}^{6+}$ ,  $\text{Pb}^{2+}$ ,  $\text{Cd}^{2+}$  and  $\text{Ni}^{2+}$  sorption onto the adsorbent was  $\text{Cr}^{6+} > \text{Pb}^{2+} > \text{Cd}^{2+} > \text{Ni}^{2+}$ .

**Keywords** Nano- $\gamma$ - $\text{Al}_2\text{O}_3$  · Adsorption · Chromium · Cadmium · Nickel · Lead

## Introduction

Heavy metal pollution occurs during different industrial activities, and rapid industrialization leads to the increase of heavy metal concentration in the environment (Rahmani et al. 2010). It can also increase the concentration of heavy metal ions, such as cadmium (Cd), lead (Pb), zinc (Zn), nickel (Ni), copper (Cu) and chromium (VI) in water resources (Aziz et al. 2008). The toxic nature of heavy metals has caused serious health problems for human, and they can accumulate in the environment (Rahmani et al. 2010). In addition, recovery and removal of heavy metals are principal purposes in industry and saving clean water resources (Sharma and Tamar 2008; Neghlani et al. 2011). Solvent extraction (Resterna et al. 2010), chemical precipitation (Soylak and Erdogan 2006; Uluzozlu et al. 2010), reverse osmosis and membrane separation (Kornilovich et al. 2000), ion exchange (Shoushtari et al. 2006), electrofloatation (Aydin and Soylok 2010), coagulation (Goncharuk et al. 2001) and adsorption process (Zhou et al. 2009) are some of the common techniques for the removal of heavy metal ions from aqueous solution. Most of these methods require either high energy or large quantities of chemicals. Adsorption method is very popular due to its simplicity and low cost (Ahn et al. 2009; Gurgel et al. 2009), and it is known to be more effective and versatile technique for heavy metal removal from aqueous solutions, especially when combined with an appropriate desorption method (Ai et al. 2008). Certain properties, such as high mechanical and thermal stability and high sorption capacity, should be considered for the adsorbent. For this reason, selection of suitable material as an adsorbent for the removal of heavy metal ions from aqueous solution would be highly important. Some of the adsorbents utilized for this purpose are carbon nanotubes (Ahmedna et al. 2004),

A. Shokati Poursani · A. H. Hassani (✉) · M. Shariat · J. Nouri  
Department of Environmental Science, Graduate School of the  
Environment and Energy, Science and Research Branch,  
Islamic Azad University, Tehran, Iran  
e-mail: hassaniamirhessam@gmail.com

A. Nilchi  
NSTRI, P.O. Box 11365-8486, Tehran, Iran

nano-metal oxides (Mohamed Mahmoud et al. 2013), nano-zeolite composites (Ngomsik et al. 2005), polymers (Baybaş and Ulusoy 2011) and polymer-metal oxides (Wu et al. 2010a, b). For example, the maximum adsorption capacities of iron oxide–alumina mixed with nano-composite fiber are found to be 90 % for Hg(II), 65 % for Ni(II), 50 % for Pb(II) and 20 % for Cu(II) (Mahapatra et al. 2013). In similar studies, the rates of adsorption onto the surface of carbon nanotubes grown on micro sized  $\text{Al}_2\text{O}_3$  particles were reported to be 10 and 1.33 mg/L for  $\text{pb}^{2+}$  and  $\text{Cd}^{2+}$ , respectively (Shu-Huei and Jao-Jia 2007). The efficiencies of adsorption by  $\text{Fe}_2\text{O}_3$ – $\text{Al}_2\text{O}_3$  nano-composite fibers were 23.7 mg/L for  $\text{Pb}^{2+}$  and 32.3 for  $\text{Ni}^{2+}$  (Mahapatra et al. 2013). In another study, adsorption efficiency was obtained to be 5 mg/L for both  $\text{Cd}^{2+}$  and  $\text{Pb}^{2+}$  (Xiadong et al. 2012). According to Hikmet and Turan (2014), the adsorption rates were found to be 15.8 mg/L for  $\text{Pb}^{2+}$  and 10.7 mg/L ( $\text{Cr}^{6+}$ ) by using Kuluncak vermiculites. Nano-structured hydrous titanium oxide has been investigated for the removal of Ni from aqueous solutions due to its physical and chemical stability, nontoxicity and high specific surface area; however, in the field of water treatment, its efficiency has not been very high leading to a low desorption rates (Debnah and Ghosh 2009). Sol–gel method is a fast, simple, reliable, convenient and low-cost technique for synthesis of nano-metal oxides. Nano-metal oxides synthesized by sol–gel technique have high surface area and monotonous particles; these properties make them very reliable with a high efficiency for the removal of heavy metal ions from aqueous solutions (Veriansyah et al. 2011; Sung Lee et al. 2012). After synthesis of nano-metal oxides by sol–gel technique with high surface area, they have found general application for removing heavy metal ions from aqueous solution. Recently,  $\text{Al}_2\text{O}_3$  nanoparticles were synthesized successfully by sol–gel technique (Yoo et al. 2009). Most of the studies, for example, on preparing nonporous iron-oxide nanoparticles, have mainly focused on synthesis, structural characterization and morphology (Mallakpoura and Baratia 2011; Wu et al. 2010a, b; Prakash et al. 2004).

In this study, a new method was applied and an organic compound (1,2-epoxybutane) was used as a precursor for synthesis in gelation process. In comparison with the frequently used sol–gel method, the advantages of this method are uniformity in size and shape of products, process time saving, simplicity of synthesis procedure and high adsorption efficiency of the nano-material. The aim of this study was to use this nano-material for the adsorption of heavy metal ions (Cr, Ni, Cd and Pb) from liquid phase under batch conditions. Structure of the synthesized nanoparticles was characterized using transmission electron microscope (TEM), X-ray diffraction (XRD) and fourier transform infrared (FTIR). Moreover, the effects of

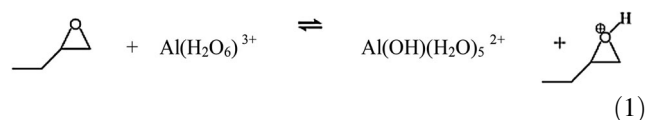
pH, contact time and adsorbent weight on adsorption process were investigated along with studying the desorption of heavy metal ions (Cr, Ni, Cd and Pb). All the experiments were carried out in laboratories of the Environment and Energy Faculty, located in Science and Research Branch of Tehran Islamic Azad University.

## Materials and methods

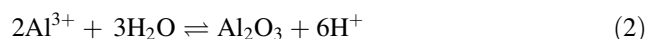
All the selected reagents were of analytical grade and purchased from Merck. The stock solutions for preparation of Cd, Ni, Cr and Pb were prepared by dissolving  $\text{Cr}_2\text{O}_7$ ,  $\text{Cd}(\text{NO}_3)_2 \cdot 11\text{H}_2\text{O}$ ,  $\text{Ni}(\text{NO}_3)_2$  and  $\text{Pb}(\text{CH}_3\text{OO})_2 \cdot 3\text{H}_2\text{O}$  in deionized water.  $\text{AlCl}_3 \cdot 6\text{H}_2\text{O}$ , 1,2-epoxybutane and  $\text{C}_2\text{H}_5\text{OH}$  were used for synthesizing nano-alumina by sol–gel method. For adjusting pH, 1 M  $\text{HNO}_3$  and  $\text{NaOH}$  solutions and Metrohm pH meter model 744 were used. Sartorius Electrical Balance Model BP 221S, Ultrasonic model Viseclean, Laboren oven, Nabertherm furnace, mixer HT Infors AG model CH-4103-BOT Tmingen, Centrifuge model MSE ministral 1000 were used for conducting the experiments, and heavy metals analysis was carried out by using ICP-Optima 2000 DV.

### Synthesis and preparation of $\gamma\text{-Al}_2\text{O}_3$

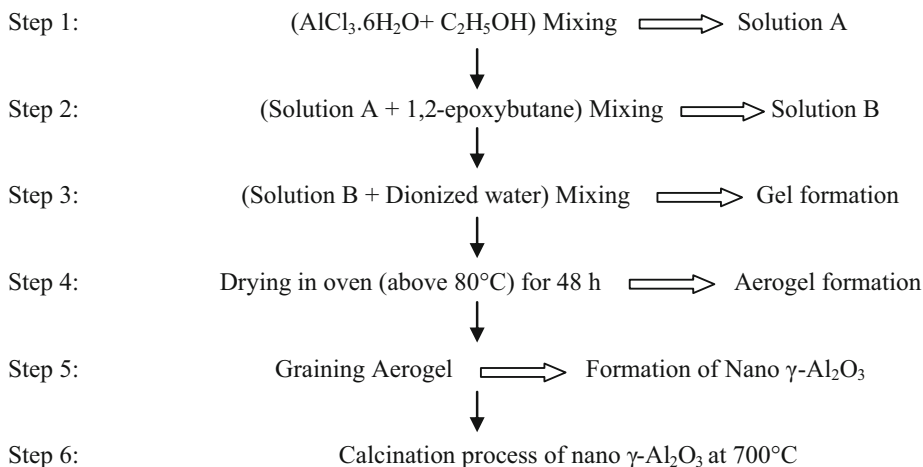
The synthesis process of nano- $\gamma\text{-Al}_2\text{O}_3$  has been presented schematically (Table 1). In the first step,  $\text{AlCl}_3 \cdot 6\text{H}_2\text{O}$  (1.25 g) was dissolved in absolute ethanol (40 mL) in a beaker by using ultrasonic for 20 min to obtain a clear solution (A). In the second step, solution (A) was mixed with 1,2-epoxybutane (5 mL) by using ultrasonic for 20 min to form solution (B). The Epoxide, when mixed with the precursor salt, acts as acid scavenger and apparently consumes protons from the hydrated Al(III) species as explained by Eq. (1):



During the third step, deionized water was added dropwise to the solution (B) until gel formation was occurred, and water acted as a gelation agent. The reaction is shown by Eq. (2) as follows:



In the fourth step, the produced gel was heated (in oven at 80 °C) to make change in aerogel mode, and then it was grained to form nano- $\gamma\text{-Al}_2\text{O}_3$ . Finally, the products were heated in a furnace (at 700 °C for 5 h) for calcination purposes to activate nanoparticle surfaces.

**Table 1** Synthesis process of nano- $\gamma$ -Al<sub>2</sub>O<sub>3</sub>

Schematic Synthesis process of  $\gamma$ -Al<sub>2</sub>O<sub>3</sub> by Sol-gel method

### Batch adsorption studies

In a single component, adsorption experiments were performed by adding 0.15 g of adsorbent to 50 mL of solution with the initial Cr<sup>6+</sup>, Pb<sup>2+</sup>, Cd<sup>2+</sup> and Ni<sup>2+</sup> ions concentration of 20 mg/L in a flask. The effect of pH on sorption ions was studied in the range of 3–6.5, at a temperature of 25 °C and contact time of 4 h. The effect of contact time was investigated by varying the time from 10 to 240 min, at a temperature of 25 °C with the obtained pH values. The effect of adsorbent weight on sorption metal ions was studied in the range of 1–4 g/L (0.05, 0.1, 0.15 and 0.2 g of adsorbent in 50 mL of metal ion solution) at the contact time of 4 h, temperature of 25 °C and the obtained pH values.

The concentration of heavy metal ions before and after equilibrium sorption was determined using inductivity coupled plasma-atomic emission spectrophotometer (ICP-AES). The uptake percentages of the heavy metal ions were calculated according to Eq. (3):

$$Up = \frac{(C_0 - C_e)}{C_0} \times 100 \quad (3)$$

where,  $C_0$  and  $C_e$  are initial and equilibrium concentrations of ions (mg/L), respectively.

## Results and discussion

### Adsorbent characterization by X-ray diffraction

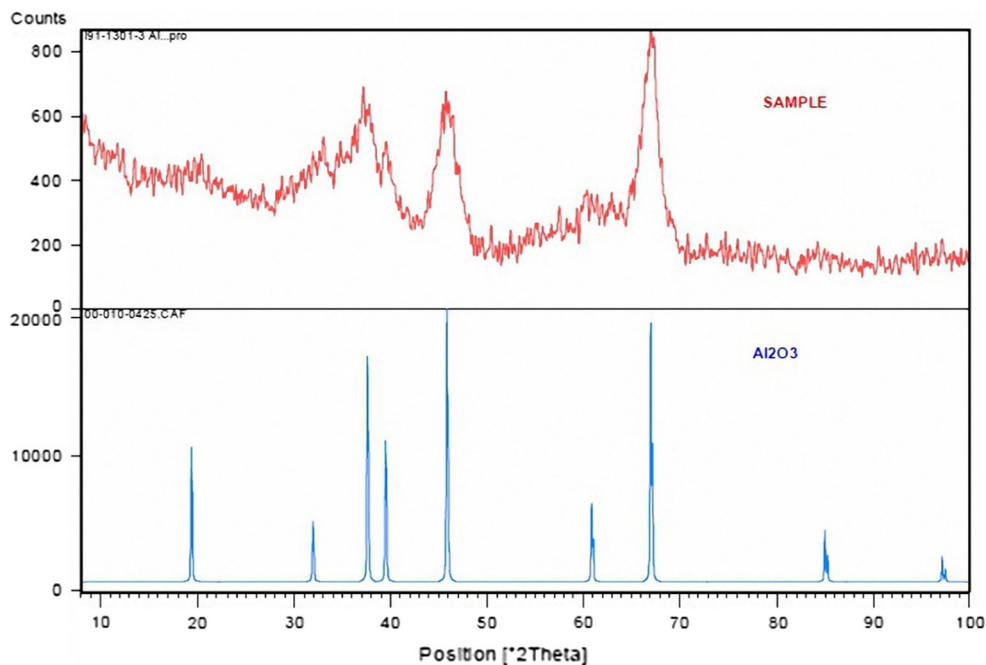
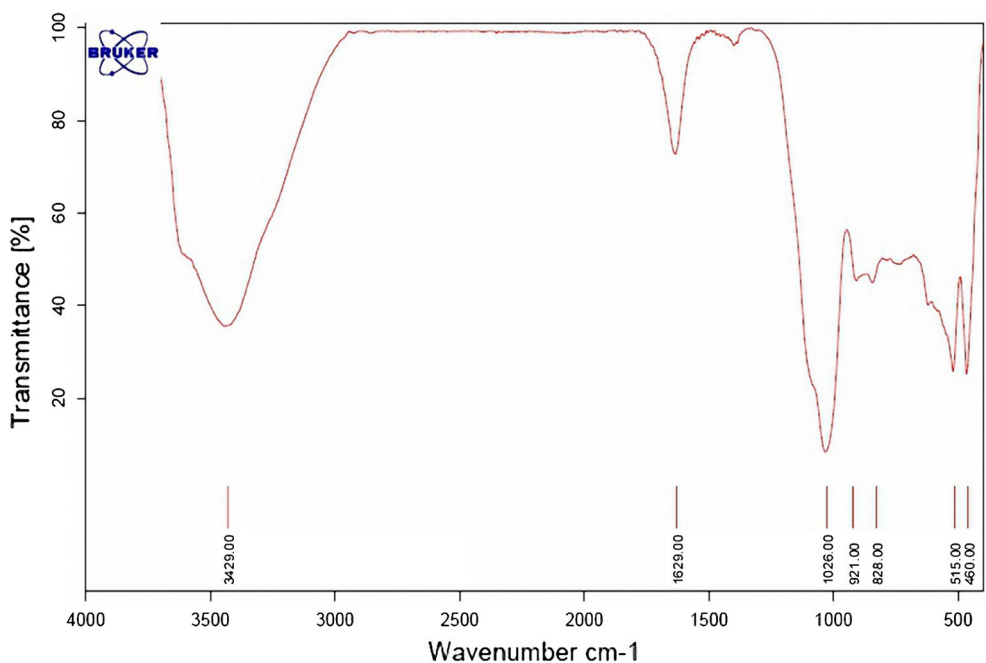
Characterization of crystalline size of the synthesized adsorbent was determined by X-ray powder diffract meter

(STV\_MP STOE Company, Germany). In this work, Cu radiation ( $\lambda_{Cu} = 1.5405 \text{ \AA}$ ) was used and the sample was scanned in a  $2\theta$  range of 8–108.5° at a scanning rate of 0.015°/S. The crystalline size was determined from the characteristic peak at  $2\theta = 67.1667^\circ$  (corresponding to the 440 plane) using Scherrer formula (Frost et al. 2013), crystalline size, nm =  $K \lambda / W \cos \theta$ , where  $K$  is the shape factor = 0.9,  $\lambda$  = wavelength of the X-ray used (1.5405) and  $W = (W_b - W_s)$ , width of peak at half-height at  $2\theta = 33.5833$  the difference of broadened profile width of the experimental sample and the standard width of reference Al<sub>2</sub>O<sub>3</sub> sample. The mean crystalline size was obtained to be 11.5 nm. Figure 1 shows the XRD graph.

### FT-IR analysis

FT-IR analysis (Vector22 Bruker Company, USA) was performed and is shown by Fig. 2. All the adsorption bands were at 3,429, 1,829, 1,026, 921, 828 and 515 cm<sup>-1</sup>. The strong IR band at 3,429 cm<sup>-1</sup> was assigned to the stretching bands of adsorbed water (Kaltchev and Tysoe 1999). The bands around the peak of 1,629 cm<sup>-1</sup> were assigned to Lewis sites, and they were also identified on dehydroxylated alumina (Nero et al. 2010). Strong band at 1,026 cm<sup>-1</sup> was tentatively ascribed to OH<sup>-</sup>-bending vibration of poorly crystalline boehmite (1,000–1,080 cm<sup>-1</sup>) (Wijnja and Schulthess 1999). The spectra of  $\gamma$ -Al<sub>2</sub>O<sub>3</sub>, the region of 1,100–950 cm<sup>-1</sup>, were obscured by the relatively strong bayerite band centered at 1,026 cm<sup>-1</sup>, and this band was assigned to one of the OH-bending ( $\gamma$ -OH) vibrations of bayerite (Parida et al. 2009). The peaks around 623 cm<sup>-1</sup> were assigned to AlO stretching of  $\gamma$ -AlO<sub>6</sub> (Zhang et al. 2008), and the bands



**Fig. 1** XRD graph of  $\gamma$ - $\text{Al}_2\text{O}_3$ **Fig. 2** FT-IR graph of synthesized  $\gamma$ - $\text{Al}_2\text{O}_3$ 

around the peaks at 667, 730 and 815  $\text{cm}^{-1}$  were due to the vibration mode of  $\text{AlO}_6$  (Ma and Zhu 2009; Ibrahim and Abu-Ayana 2009). The bands around 775 and 590  $\text{cm}^{-1}$  were generally associated with the stretching vibration of  $\text{AlO}$  bond of four and six coordinated Al in  $\gamma$ - $\text{Al}_2\text{O}_3$  (Zhou and Antonietti 2007; Padmaja et al. 2001). The bands in the range of 500–750  $\text{cm}^{-1}$  were related to the stretching vibrations of  $\text{AlO}$  bonds of the octahedrally coordinated Al. The bands resulted from vibrations of  $\text{AlO}$  bond in  $\text{AlO}_4$

units were presented around 750–900  $\text{cm}^{-1}$  (Okada et al. 1991; Rodriguez et al. 2013).

#### TEM images

The TEM images (taken by PHILIPS, EM 208) of synthesized nano- $\text{Al}_2\text{O}_3$  are illustrated in Fig. 3. It can be noticed that the nanoparticles are very aggregate and that they have a mean diameter of about 11.5 nm. In the present



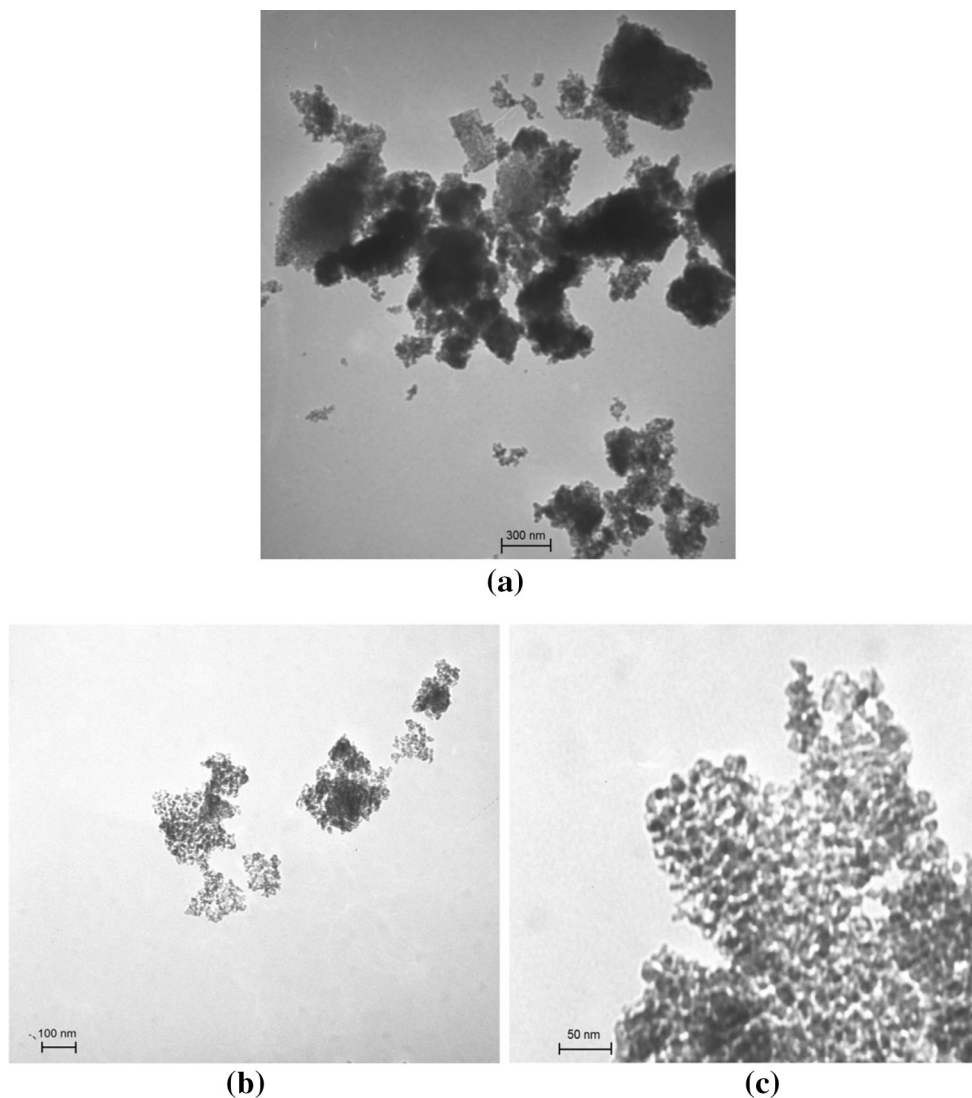


**Fig. 3** TEM images of  $\gamma$ - $\text{Al}_2\text{O}_3$  nanoparticles, **a** magnification of 300 nm, **b** magnification of 100 nm, **c** magnification of 50 nm

context, the discrepancy between the X-ray crystallite size and that measured in the TEM can be interpreted as being due to lattice distortions in the prepared powder. As a result of a sub-structure much smaller than the nano-crystalline, the grain size measured in the TEM is in good agreement with the findings of Chandramouli et al. (1996).

#### Surface areas and pore volumes

Brunauer–Emmett–Teller (BET) specific surface area was determined through nitrogen adsorption isotherms using Quantachrome NOVA 2200e system. Using the BET method, the surface area of the sample was calculated to be  $125.4 \text{ m}^2/\text{g}$ . Also, the pore size distribution attained by Barrett–Joyner–Halenda (BJH method revealed the mesoporosity. The pore size obtained by this method was 8.92 nm.

#### Adsorption properties of $\gamma$ - $\text{Al}_2\text{O}_3$

##### *Effect of pH*

Optimizing the initial pH value of the adsorption is an important parameter that seeks to obtain high adsorption capacity. The effect of pH on the adsorption of heavy metal ions is shown in Fig. 4. The pH range for this study was selected to be 3–6.5 based on previous studies (Asencios and S-Kou 2012; Sen and Sarzali 2008). A very low adsorption rate was observed at the pH below 3 (Mahapatra et al. 2013). At low pH values, the sorbent surface would be closely associated with  $\text{H}_3\text{O}^+$  which binds the access of metal ions to the surface of adsorbent. At pH levels of 3 (Cr) and 5 (Ni, Cd and Pb), the amount of heavy metal ion sorption onto the adsorbent (nano-structure of  $\text{Al}_2\text{O}_3$ ) increased with the increase of pH because the competition



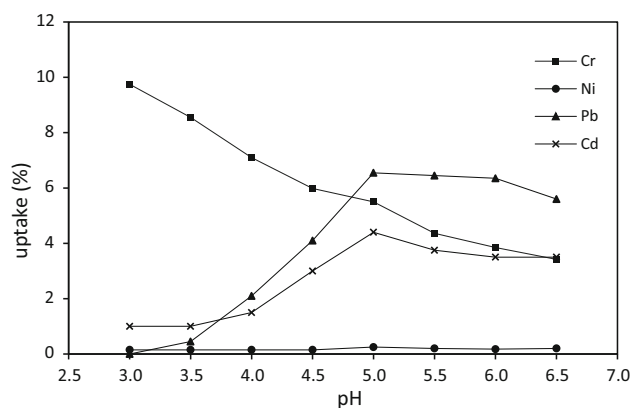


**Fig. 4** Effect of pH value on adsorption of  $\text{Cr}^{6+}$ ,  $\text{Ni}^{2+}$ ,  $\text{Cd}^{2+}$  and  $\text{Pb}^{2+}$  onto  $\gamma\text{-Al}_2\text{O}_3$ . Conditions: adsorbent weight 3 g/L, adsorption time 2 h

between hydrogen ion and metal ions decreased. The adsorption capacity of Ni, Cd and Pb ions reached a maximum with the pH of 5.0; however, the maximum adsorption capacity of Cr ions was obtained at pH of 3.0. The maximum adsorption for  $\text{Cr}^{6+}$  ions was obtained at  $\text{pH} = 3$  (95 %). As can be seen in Fig. 4, adsorption of  $\text{Cd}^{2+}$  and  $\text{Pb}^{2+}$  ions increases up to  $\text{pH} = 5$ . The adsorption of  $\text{Ni}^{2+}$  is low (<4 %) at all investigated pH values. However, the sorption capacity decreased with further increase of pH value.

Since the selectivity of adsorption varies as  $\text{Cr}^{6+} > \text{Pb}^{2+} > \text{Cd}^{2+} > \text{Ni}^{2+}$ , pHs of 3.0 (for  $\text{Cr}^{6+}$ ) and 5.0 (for  $\text{Ni}^{2+}$ ,  $\text{Pb}^{2+}$  and  $\text{Cd}^{2+}$ ) were chosen for the following experiments.

#### Effect of time contact

The effect of time on the adsorption of ions by nano-structured  $\gamma\text{-Al}_2\text{O}_3$  was studied. Adsorption of  $\text{Cr}^{6+}$ ,  $\text{Ni}^{2+}$ ,  $\text{Cd}^{2+}$  and  $\text{Pb}^{2+}$  ions from aqueous solutions, which was adjusted to the nano-structured  $\gamma\text{-Al}_2\text{O}_3$  (0.15 g) at optimum pHs, was studied at different shaking times in the range of 10–240 min (Fig. 5). The removal efficiency of all ions reached the maximum value after 4 h. This could be due to the fact that initially all adsorbent sites were vacant and the solute concentration gradient was high. Therefore, based on the results, a contact time of 4 h was selected in subsequent studies. The results indicated that within 4 h of shaking,  $\text{Cr}^{6+}$  ions were totally removed from aqueous solution. In similar experimental conditions, 75 % of  $\text{Pb}^{2+}$  ions were removed.

#### Effect of amount of adsorbent

The effect of adsorbent amount on adsorption rate was examined by a series of experiments performed by using

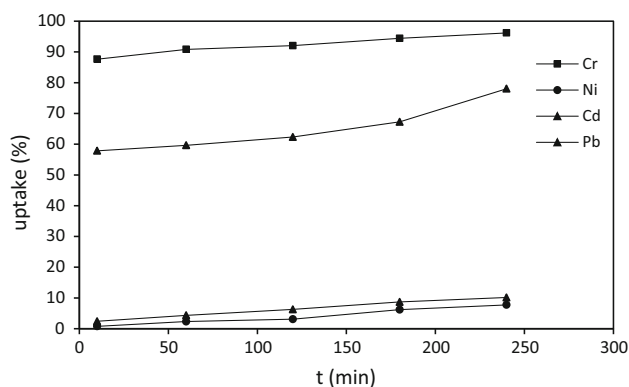


**Fig. 5** Effect of time on adsorption of  $\text{Cr}^{6+}$ ,  $\text{Ni}^{2+}$ ,  $\text{Cd}^{2+}$  and  $\text{Pb}^{2+}$  onto  $\gamma\text{-Al}_2\text{O}_3$ . Conditions: adsorbent weight of 3 g/L at optimum pH values

different amounts of synthesized  $\gamma\text{-Al}_2\text{O}_3$  (0.05, 0.1, 0.15 and 0.2 g) (Fig. 6). The maximum uptakes attained after using 0.2 g of adsorbent were 99.99 % for  $\text{Cr}^{3+}$  and 80 % for  $\text{Pb}^{2+}$ .

#### High adsorption efficiency

The results showed the high adsorption efficiency of synthesized nano- $\gamma\text{-Al}_2\text{O}_3$  for  $\text{Cr}^{3+}$  and  $\text{Pb}^{2+}$ . It could be related to the uniformity of size and shapes of nanoparticles as a result of applying a novel synthesis technique.

#### Desorption studies

The aqueous solutions (50 mL) containing the studied heavy metal ions (20 mg/L) under the optimum experimental condition were magnetically stirred with 0.15 g of the adsorbent for 240 min at 25 °C. Then, desorption studies were carried out using 50 mL of 1 M  $\text{HNO}_3$  during 1-h mixing. It was found that the adsorbed ions could be

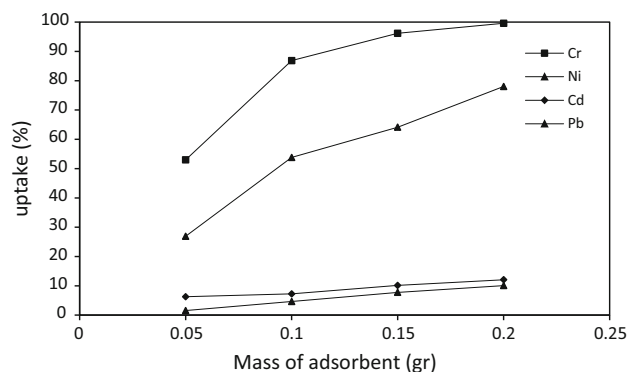


**Fig. 6** Effect of mass adsorbent value on adsorption of  $\text{Cr}^{6+}$ ,  $\text{Ni}^{2+}$ ,  $\text{Cd}^{2+}$  and  $\text{Pb}^{2+}$  onto  $\gamma\text{-Al}_2\text{O}_3$ . Conditions: adsorption time of 4 h at optimum pH values



quantitatively stripped by contacting nitric acid (Table 2). Finally, desorption of heavy metal ions from the surface of adsorbent was done, and the results showed the high efficiency of desorption rate.

**Kinetic study**

Figure 5 indicates the variation of amounts of Cr<sup>3+</sup>, Ni<sup>2+</sup>, Cd<sup>2+</sup> and Pb<sup>2+</sup> ions adsorbed at different time intervals for a fixed initial ion concentration of 20 mg/L. The data revealed that the amount of adsorbed ions studied increased with the increase of contact time. To describe changes in sorption of metal ions with time, two simple kinetic models were tested. The experimental kinetic data for Cr<sup>6+</sup>, Pb<sup>2+</sup>, Cd<sup>2+</sup> and Ni<sup>2+</sup> ions adsorption from aqueous solutions on the γ-Al<sub>2</sub>O<sub>3</sub> nanoparticles were modeled using pseudo-first- and pseudo-second-order kinetic models. In order to investigate the accuracy of these models in predicting the Cr<sup>6+</sup>, Pb<sup>2+</sup>, Cd<sup>2+</sup> and Ni<sup>2+</sup> ions' adsorption behavior, the correlation coefficient (*R*) of each model, which is an important factor, was used. The success of the models in predicting the kinetics of adsorbate sorption is described by a relatively high *R* value (Nilchi et al. 2012). The rate constant of each metal ion removal from the solution by nano-γ-Al<sub>2</sub>O<sub>3</sub> was also determined using pseudo-first-order and pseudo-second-order rate models. The Lagergren's pseudo-first-order expression is given by Eq. (4) (Langmuir 1916):

$$\log(q_e - q_t) = \log q_e - \frac{k_1}{2.303} t \tag{4}$$

where *q<sub>e</sub>* and *q<sub>t</sub>* are the amounts of metals adsorbed on the sorbent (mg/g) at equilibrium and at time *t*, respectively, and *k<sub>1</sub>* is the rate constant of the first-order adsorption (min<sup>-1</sup>). The straight line plots of (*q<sub>e</sub>* - *q<sub>t</sub>*) against *t* were used to determine the rate constant, *k<sub>1</sub>* and correlation coefficient; *R*<sup>2</sup> values of the metals were calculated from these plots. The calculated correlation coefficient for pseudo-first-order and the values of constants are shown in Table 3. The pseudo-second-order rate model is expressed by Eq. (5) (Aksu 2002):

$$\frac{t}{q_t} = \frac{1}{k_2 q_e^2} + \frac{t}{q_e} \tag{5}$$

where *K<sub>2</sub>* is the rate constant of adsorption (g/mg/min), *q<sub>e</sub>* is the amount adsorbed at equilibrium, and *q<sub>t</sub>* is the amount adsorbed at any time. The equilibrium adsorption amount

**Table 2** Desorption studies of the studied ions from surface γ-Al<sub>2</sub>O<sub>3</sub> nanoparticles

Metal ion	Cr <sup>6+</sup>	Pb <sup>2+</sup>	Cd <sup>2+</sup>	Ni <sup>2+</sup>
Adsorption	99.99 %	80 %	10.14 %	7.75 %
Desorption	95 %	94 %	94 %	92 %

**Table 3** Calculated parameters of the pseudo-first-order and pseudo-second-order kinetic models for Cr<sup>6+</sup>, Ni<sup>2+</sup>, Cd<sup>2+</sup> and Pb<sup>2+</sup> ions adsorbed onto nano-γ-Al<sub>2</sub>O<sub>3</sub>

	Pseudo-first-order			Pseudo-second-order		
	<i>q<sub>e</sub></i> (mg/g)	<i>K<sub>1</sub></i> (min <sup>-1</sup> )	<i>R</i> <sup>2</sup>	<i>q<sub>e</sub></i> (mg/g)	<i>K</i> <sup>2</sup> (g/mg/min)	<i>R</i> <sup>2</sup>
Cr <sup>6+</sup>	0.570	0.020	0.759	8.130	0.030	0.999
Pb <sup>2+</sup>	3.270	0.010	0.656	5.780	12.400	0.978
Cd <sup>2+</sup>	0.870	0.010	0.905	0.880	0.013	0.875
Ni <sup>2+</sup>	0.190	0.001	0.037	0.650	0.005	0.875

(*q<sub>e</sub>*) and the pseudo-second-order rate parameters (*K<sub>2</sub>*) can be calculated from the slope and intercept of *t/q<sub>t</sub>* plotted versus *t*. The values of constants and calculated correlation coefficients for pseudo-second-order are presented in Table 3.

In adsorption of Cr<sup>6+</sup>, Pb<sup>2+</sup> and Ni<sup>2+</sup> ions, correlation coefficient for the pseudo-second-order equation was larger than that of the pseudo-first-order equation, indicating that Cr<sup>6+</sup>, Pb<sup>2+</sup> and Ni<sup>2+</sup> ions adsorption onto the synthesized γ-Al<sub>2</sub>O<sub>3</sub> nanoparticles follows the pseudo-second-order kinetic model. It was observed that the predicted *q<sub>e</sub>* value for the pseudo-second-order model agreed well with the experimental value. Adsorption of Cd<sup>2+</sup> ions onto adsorbent particles followed the pseudo-first-order kinetic model, implying that the predicted *q<sub>e</sub>* value for the pseudo-first-order model agreed well with the experimental value. Therefore, the pseudo-second-order kinetic model was more suitable for predicting the kinetic sorption process of Cr<sup>6+</sup>, Pb<sup>2+</sup> and Ni<sup>2+</sup> ions, whereas pseudo-first-order kinetic model was competent for predicting the kinetic sorption process of Cd<sup>2+</sup> onto the synthesized γ-Al<sub>2</sub>O<sub>3</sub> nanoparticles (Table 3). The best-fitted plots are illustrated in Fig. 7.

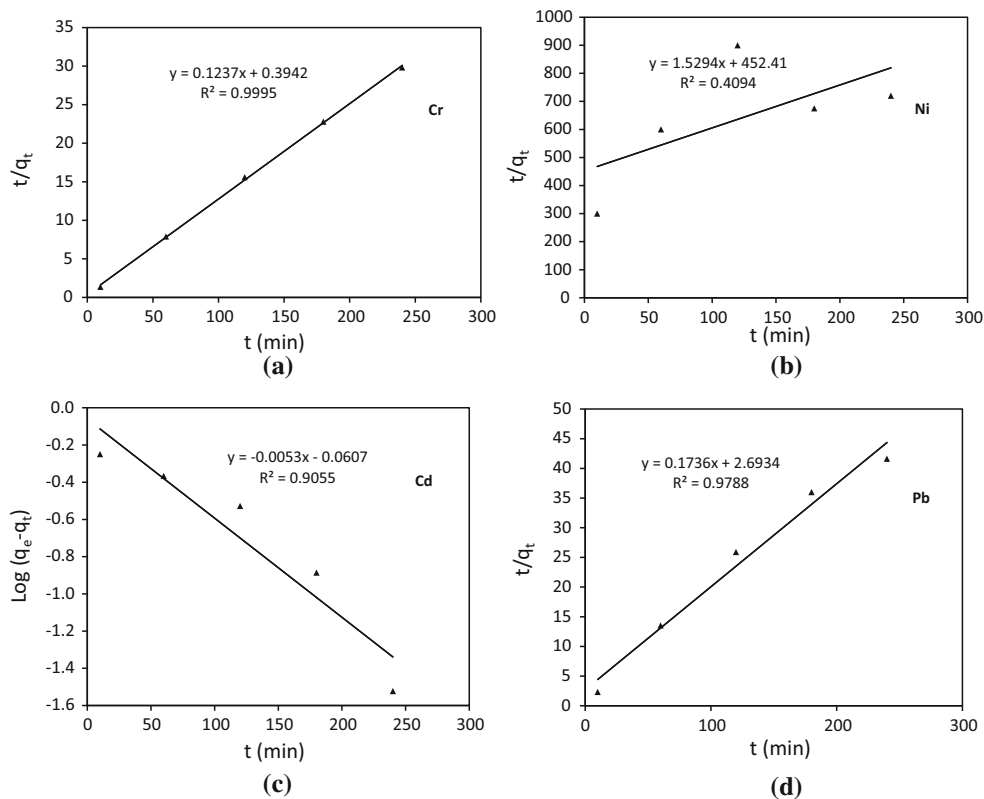
**Adsorption isotherms**

Adsorption equilibrium is usually described by an isotherm equation whose parameters express the surface properties and affinity of the sorbent at a fixed temperature and pH. An adsorption isotherm describes the relationship between the amount of adsorbate on the adsorbent and the concentration of dissolved adsorbate in the liquid at equilibrium. In this concern, the adsorption isotherms for the removal of Cr<sup>6+</sup>, Ni<sup>2+</sup>, Cd<sup>2+</sup> and Pb<sup>2+</sup> ions from aqueous solutions onto synthesized nano-γ-Al<sub>2</sub>O<sub>3</sub> were determined. Figure 8 shows, as a sample, the experimental and isotherm data fitted by Langmuir and Freundlich isotherm models at 298 K.

**Langmuir isotherm model**

Langmuir sorption isotherm models the monolayer coverage of the sorption surfaces and assumes that sorption

**Fig. 7** Pseudo-second-order kinetic plots for **a** Cr<sup>6+</sup>, **b** Ni<sup>2+</sup> and **d** Pb<sup>2+</sup>, and pseudo-first-order kinetic plot for **c** Cd<sup>2+</sup> sorption ions adsorbed onto nano- $\gamma$ -Al<sub>2</sub>O<sub>3</sub>



occurs on a structurally homogeneous adsorbent, and all the sorption sites are energetically identical. The linearized form of the Langmuir equation is given by Eq. (6) (El-Kamash 2008):

$$\frac{C_e}{q_e} = \frac{1}{q_{\max}b} + \frac{C_e}{q_{\max}} \quad (6)$$

where  $q_{\max}$  is the maximum sorption capacity (mg/g), and  $b$  is a constant related to binding energy of the sorption system (l/mg). The graphic presentations of  $(C_e/q_e)$  versus  $C_e$  give straight lines that the numerical value of constants  $q_{\max}$  and  $b$  evaluated from the slope and intercept of plots (Table 4).

#### Freundlich isotherm

Freundlich equation is derived to model the multilayer sorption and for the sorption on heterogeneous surfaces. The logarithmic form of Freundlich equation can be described by Eq. (7) (El-Kamash 2008):

$$\log q_e = \log K_f + \frac{1}{n} \log C_e \quad (7)$$

where  $K_f$  is a constant indicative of the relative sorption capacity of nano- $\gamma$ -Al<sub>2</sub>O<sub>3</sub> (mg/g), and  $1/n$  is a constant indicative of the intensity of sorption process. The numerical values of the constants  $1/n$  and  $K_f$  are computed from the slope and the intercepts of  $q_e$  versus  $\log C_e$  curve. The correlation coefficient and other parameters obtained for the adsorbent are given in Table 4.

#### Tempkin isotherm

The Tempkin equation is explained by Eq. (8) (El-Kamash 2008):

$$q_e = \frac{RT}{b} \ln(aC_e) \quad (8)$$

where  $R$  is the gas constant (0.0083 kJ/K mol),  $T$  is the absolute temperature (K),  $b$  is the Tempkin constant related to the heat of sorption (kJ/mol), and  $a$  is the Tempkin isotherm constant (L/g). Drawing  $q_e$  versus  $\ln(C_e)$  allows for evaluating  $a$ ,  $b$  and the corresponding  $R^2$  of the results (Table 4).





**Fig. 8** Langmuir adsorption isotherm plots for the sorption of (a) Cr<sup>6+</sup>, (b) Ni<sup>2+</sup> and (d) Pb<sup>2+</sup> ions, and Freundlich plot for (c) Cd<sup>2+</sup> ions

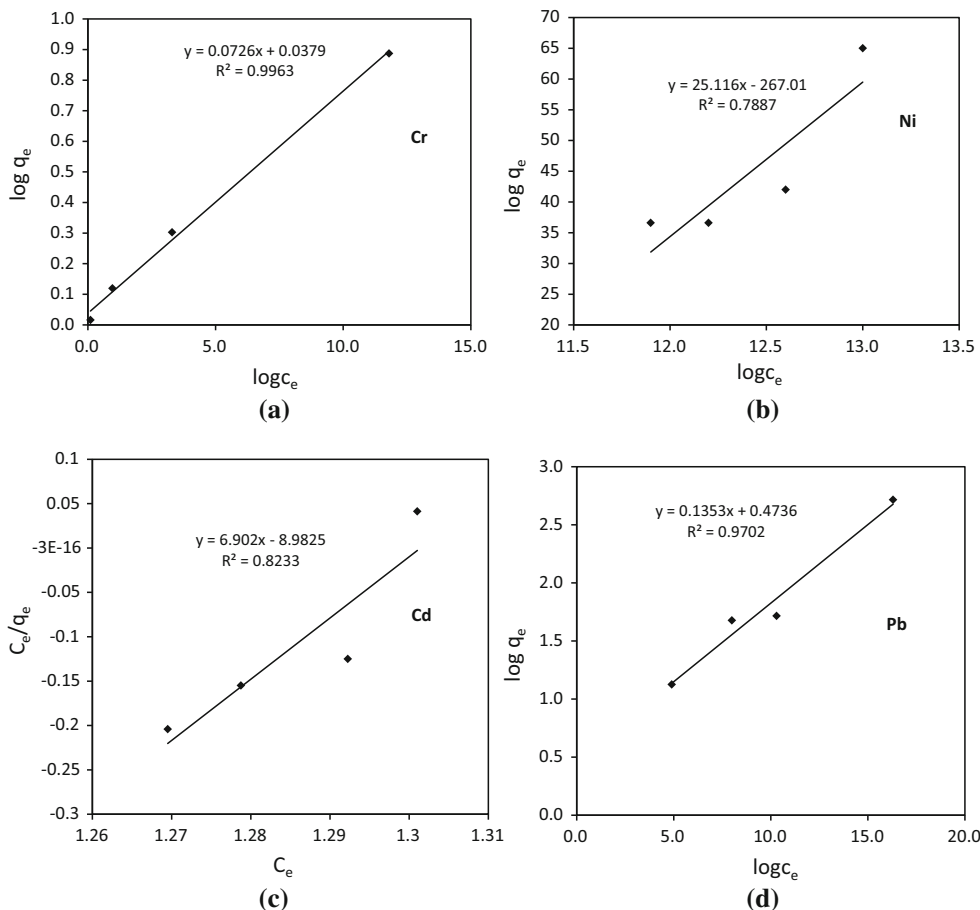


**Table 4** Parameters of Langmuir, Freundlich and Temkin isotherms for the studied ions sorption onto nano- $\gamma$ -Al<sub>2</sub>O<sub>3</sub>

Isotherm equations	Parameters	Cr <sup>6+</sup>	Pb <sup>2+</sup>	Cd <sup>2+</sup>	Ni <sup>2+</sup>
Langmuir	$q_{max}$ (mg/g)	13.89	7.39	-0.138	0.04
	$b$ (L/mg)	1.95	0.29	0.044	-0.09
	$R^2$	0.996	0.970	0.816	0.788
Freundlich	$K_f$ (mg/g)	8.75	2.73	0.13	$3.13 \times 10^5$
	$n$	6.21	0.38	0.14	-0.19
	$R^2$	0.974	0.821	0.823	0.754
Temkin	$a$ (L/g)	464.42	3.537	0.06	0.065
	$b$ (kJ/mol)	4.56	1.62	0.43	-1.76
	$R^2$	0.945	0.810	0.78	0.78

Comparison of  $R^2$  values presented in Table 4 results in selecting the appropriate adsorption isotherm model describing the adsorption process of the studied ion by

nano- $\gamma$ -Al<sub>2</sub>O<sub>3</sub>.  $R^2$  value close to 1 is indicative of the suitability of this model for describing the experimental data (Shiri-Yekta et al. 2013). This comparison reveals that the adsorption process isotherms of Cr<sup>6+</sup> ( $R^2 = 0.99$ ), Pb<sup>2+</sup> ( $R^2 = 0.97$ ) and Ni<sup>2+</sup> ( $R^2 = 0.79$ ) ions can be more suitably described by the Langmuir and Cd<sup>2+</sup> ( $R^2 = 0.82$ ) ions to be described by Freundlich model (Fig. 8). The experimental results showed that Cr<sup>6+</sup> and Pb<sup>2+</sup> were adsorbed onto  $\gamma$ -Al<sub>2</sub>O<sub>3</sub> in greater amounts than Ni<sup>2+</sup> and Cd<sup>2+</sup>. The results of  $Q_{max}$  and  $K_f$  values in Langmuir and Freundlich isotherms show the capability of sorption on an adsorbent. Comparing the quantities presented in Table 4, adsorption rates of Cr<sup>6+</sup>, Pb<sup>2+</sup>, Cd<sup>2+</sup> and Ni<sup>2+</sup> onto  $\gamma$ -Al<sub>2</sub>O<sub>3</sub> were found to be 13.89, 7.39, 0.13 and 0.04 mg/g, respectively.

The Langmuir isotherm well fitted to the experimental data, seemingly due to the homogeneous distribution of active sites on nano-structure of Al<sub>2</sub>O<sub>3</sub> adsorbent. Based on

Langmuir model assumptions, adsorption energies are uniform and independent of surface coverage, and complete coverage of the surface by a monolayer of adsorbate indicates maximum adsorption. The Freundlich well fitted to the experimental data, seemingly due to the heterogeneous distribution of active sites on nano-structure of  $\text{Al}_2\text{O}_3$  adsorbent. Based on Freundlich assumption, adsorbing surface is energetically heterogeneous, consisting of adsorption sites of differing energies.

## Conclusion

The experimental results indicate that nano-structured  $\gamma\text{-Al}_2\text{O}_3$  synthesized by sol-gel method can be an effective adsorbent for the adsorption of  $\text{Cr}^{6+}$  and  $\text{Pb}^{2+}$  in comparison with  $\text{Cd}^{2+}$  and  $\text{Ni}^{2+}$  ions from aqueous solutions under optimized conditions of pH (3 and 5 for  $\text{Cr(VI)}$  and  $\text{Pb(II)}$ , respectively), adsorbent weight (3 g/L), contact time (4 h) and in room temperature (25 °C). All kinetic results suggest that sorption of Cr, Ni and Pb by nano-structured  $\gamma\text{-Al}_2\text{O}_3$  followed the second-order kinetics model and that sorption of Cd by adsorbent followed the first-order kinetics model relying on an assumption that sorption might be a rate-limiting step involving valence forces through sharing or exchange of electrons between adsorbent and sorbent. The adsorption isotherms for Cr, Ni and Pb well fitted to the Langmuir adsorption isotherm equations, while the adsorption isotherms for Cd well fitted to the Freundlich adsorption isotherm equations. The maximum capacities of adsorbent were 13.3 mg/g for  $\text{Cr}^{6+}$ , 0.33 mg/g for  $\text{Ni}^{2+}$ , 1.1 mg/g for  $\text{Cd}^{2+}$  and 6 mg/g for  $\text{Pb}^{2+}$ , respectively. Comparing this work with similar projects shows that heavy metal ion (Cr and Pb) removal by synthesized nano- $\text{Al}_2\text{O}_3$  is very high and that the synthesized adsorbent would be reusable with high efficiency after desorption process. The nano-structure of  $\gamma\text{-Al}_2\text{O}_3$  exhibited a good capability to be used in water and wastewater treatment for removal of Cr and Pb.

**Acknowledgments** The authors wish to extend their sincere gratitude to all who supported this work.

## References

- Ahmedna M, Marshall WE, Husseiny AA, Rao RM, Goktepe I (2004) The use of nutshell carbons in drinking water filters for removal of trace metal. *Water Res* 38(4):1062–1068
- Ahn CK, Park D, Woo SH, Park JM (2009) Removal of cationic heavy metal from aqueous solution by activated carbon impregnated with anionic surfactants. *J Hazard Mater* 164:1130–1136
- Ai ZH, Chen Y, Zhang LZ, Qiu JR (2008) Efficient removal of  $\text{Cr(VI)}$  from aqueous solution with  $\text{Fe@Fe}_2\text{O}_3$  core-shell nanowires. *J Environ Sci Technol* 42:6955–6960
- Aksu Z (2002) Determination of the equilibrium, kinetic and thermodynamic parameters of the batch biosorption of nickel(II) ions onto *Chlorella vulgaris*. *Prog Biochem* 38(1):89–99
- Asencios YJO, S-Kou MR (2012) Synthesis of high surface  $\gamma\text{-Al}_2\text{O}_3$  from aluminum scrap and its use for the adsorption of metals:  $\text{Pb(II)}$ ,  $\text{Cd(II)}$  and  $\text{Zn(II)}$ . *Appl Surf Sci* 258:10002–10011
- Aydin FA, Soylak M (2010) Separation, pre concentration and inductively coupled plasma-mass spectrometric (ICP-MS) determination of thorium (IV), titanium (IV), iron (III), lead (II) and chromium (III) on 2-nitroso-1-naphthol Impregnated MCI GEL CHP20P resin. *J Hazard Mater* 173:669–674
- Aziz HA, Adlan MN, Ariffin KS (2008) Heavy metals (Cd, Pb, Zn, Ni, Cu and  $\text{Cr(III)}$ ) removal from water in Malaysia: post treatment by high quality limestone. *Bioresour Technol* 99:1578–1583
- Baybaş D, Ulusoy U (2011) The use of polyacrylamide-aluminosilicate composites for thorium adsorption. *J Appl Clay Sci* 5:138–146
- Chandramouli V, Anthonysamy S, Vasudeva Rao PR, Divakar R (1996) PVA aided microwave synthesis: a novel route for the production of nanocrystalline thoria powder. *J Nucl Mater* 231:213–220
- Debnah S, Ghosh UC (2009) Nano structured hydrous titanium (IV) oxide: synthesis, characterization and Ni (II) adsorption behavior. *J Chem Eng* 152:480–491
- El-Kamash AM (2008) Evaluation of zeolite A for the sorptive removal of  $\text{Cs}^+$  and  $\text{Sr}^{2+}$  ions from aqueous solutions using batch and fixed bed column operations. *J Hazard Mater* 151:432–445
- Frost RL, Scholz R, Lopes A, Xi Y, Gobac ZI (2013) LFC. Horta, Raman and infrared spectroscopic characterization of the phosphate mineral paravauxite  $\text{Fe}^{2+}\text{Al}_2(\text{PO}_4)_2(\text{OH})_2 \cdot 8\text{H}_2\text{O}$ . *Spectrochim Acta A* 116:491–496
- Goncharuk VV, Kornilovich BY, Pavlenko VM, Babak MI, Pshinko GN, Pysmennyi BV, Kovalchuk IA, Safronova VG (2001) Uranium compounds purification from water and wastewater. *J Water Chem Technol* 23:44–50
- Gurgel LVA, Melo JCPD, De Lena JC, Gil LF (2009) Adsorption of chromium (VI) ion from aqueous solution by succinylated mercerized cellulose functionalized with quaternary ammonium groups. *J Bioresour Technol* 100(13):3214–3220



- Hikmet S, Turan U (2014) Removal of heavy metal ions from aqueous medium using Kuluncak (Malatya) vermiculites and effect of precipitation on removal. *J Appl Clay Sci* 95:1–8
- Ibrahim DM, Abu-Ayana YM (2009) Preparation of nano alumina via resin synthesis. *Mater Chem Phys* 113(2–3):579–586
- Kaltchev M, Tysoe WT (1999) An infrared spectroscopic investigation of thin alumina films: measurement of acid sites and surface reactivity. *J Surf Sci* 430:29–36
- Kornilovich BY, Kovalchuk IA, Pshinko GN, Tsapyuk EA, Krivoruchko AP (2000) Water purification of uranium by the method of ultrafiltration. *J Water Chem Technol* 22:43–47
- Langmuir I (1916) The constitution and fundamental properties of solids and liquids. Part I. Solids. *J Am Chem Soc* 38(11):2221–2295
- Ma MG, Zhu JF (2009) A facile solvo thermal route to synthesis of  $\gamma$ -alumina with bundle-like and flower-like morphologies. *Mater Lett* 63:881–883
- Mahapatra A, Mishra BG, Hota G (2013) Electrospun  $\text{Fe}_2\text{O}_3$ - $\text{Al}_2\text{O}_3$  nanocomposite fibers as efficient adsorbent for removal of heavy metal ions from aqueous solution. *J Hazard Mater* 258–259:116–123
- Mohamed Mahmoud E, Mohamed Abdelwahab S, Fathallah ME (2013) Design of novel nano-sorbents based on nano-magnetic iron oxide-bound-nano-silicon oxide-immobilized-triethylene-tetramine for implementation in water treatment of heavy metals. *Chem Eng J* 223:318–327
- Mallakpoura Sh, Baratia A (2011) Efficient preparation of hybrid nanocomposite coatings based on poly (vinyl alcohol) and silane coupling agent modified  $\text{TiO}_2$  nanoparticles. *Prog Org Coat* 71:391–398
- Neghlani PK, Rafizadeh M, Taromi FA (2011) Preparation of aminated-polyacrylonitril nano fiber membranes for the adsorption of metal ions: comparison with microfiber. *J Hazard Mater* 186:182–189
- Nero MD, Galindo C, Barillon RI, Halter E, Made B (2010) Surface reactivity of  $\alpha$ - $\text{Al}_2\text{O}_3$  and mechanisms of phosphate sorption: in situ ATR-FTIR spectroscopy and potential studies. *J Colloid Interface Sci* 342:437–444
- Ngomsik AF, Bee A, Draye M, Cote G, Cabuil V (2005) Magnetic nano- and microparticles for metal removal and environmental applications. *J Comput Ren Chem* 8(6–7):963–970
- Nilchi A, Saberi R, Azizpour H, Moradi M, Zarghami R, Naushad M (2012) Adsorption of caesium from aqueous solution using cerium molybdate-pan composite. *Chem Ecol* 28(2):169–185
- Okada AK, Otsuka N, Somiya S (1991) Review of mullite synthesis routes in Japan. *Am Ceram Soc Bull* 70:1633–1640
- Padmaja P, Anilkumar GM, Mukindan P, Aruldas G, Warriar KGK (2001) Characterization of stoichiometric sol-gel mullite by Fourier transform infrared spectroscopy. *Int J Inorg Mater* 3:693–698
- Parida KM, Pradhan AC, Das J, Sahu N (2009) Synthesis and characterization of nanosized porous gamma-alumina by control precipitation method. *J Mater Chem Phys* 113:244–248
- Prakash A, McCormick AV, Zachariah MR (2004) Aero-sol-gel synthesis of nano porous iron-oxide particles: a potential oxidizer for nano energetic materials. *J Chem Mater* 16:1466–1471
- Rahmani A, Mousavi HZ, Fazli M (2010) Effect of nanostructure alumina on adsorption of heavy metals. *J Desalin* 253:94–100
- Resterna AB, Cierpiszewski R, Prochaska K (2010) Kinetic and equilibrium studies of the removal of cadmium ions from acidic chloride solutions by hydrophobic pyridinecarboxamide extractants. *J Hazard Mater* 179:828–833
- Rodriguez M, Sifontes AB, Mendez FJ, Diaz Y, Izalesb EC, Brito JL (2013) Template synthesis and characterization of mesoporous  $\gamma$ - $\text{Al}_2\text{O}_3$  hollow nano rods using *Stevia rebaudiana* leaf aqueous extract. *J Ceram Int* 39:4499–4506
- Sen TK, Sarzali MV (2008) Removal of cadmium metal ion ( $\text{Cd}^{2+}$ ) from its aqueous solution by aluminium oxide ( $\text{Al}_2\text{O}_3$ ): a kinetic and equilibrium study. *Chem Eng J* 142:256–262
- Sharma P, Tamar R (2008) Synthesis and application of an analogue of desolate for the removal of Uranium (VI), Thorium(IV), and europium(III) from aqueous waste. *Micropor Mesopor Mater* 116:641–652
- Shiri-Yekta Z, Yaftian MR, Nilchi A (2013) Silica nanoparticles modified with a Schiff base ligand: an efficient adsorbent for Th(IV), U(VI) and Eu(III) ions. *Korean J Chem Eng* 30(8):1644–1651
- Shoushtari AM, Zargaran M, Abdouss M (2006) Preparation and characterization of high efficiency ionexchange cross linked acrylic fibers. *J Appl Polym Sci* 101:2202–2209
- Shu-Huei H, Jao-Jia H (2007) Adsorption behavior of heavy metal ions by carbon nanotube grown on microsized  $\text{Al}_2\text{O}_3$  particles. *J Univ Sci Technol B* 14(1):77–84
- Soylak M, Erdogan ND (2006) Copper (II)-rubeanic acid co precipitation system for separation-preconcentration of trace metal ions in environmental samples for their flame atomic absorption spectrometric determinations. *J Hazard Mater* 137:1035–1041
- Sung Lee J, Soo Kim H, Su Lee J, Park NK, Lee TJ, Kang M (2012) Synthesis of  $\alpha$ - $\text{Al}_2\text{O}_3$  at mild temperatures by controlling aluminum precursor, pH, and ethylene diamine chelating additive. *Ceram Int* 38:6685–6691
- Uluozlu OD, Tuzen M, Mendil D, Soy lak M (2010) Co-precipitation of trace elements with  $\text{Ni}^{2+}$ /2-nitroso-1-naphthol-4-sulfonic acid and their determination by flame atomic absorption spectrometry. *J Hazard Mater* 176:032–1037
- Veriansyah B, Susanti RF, Nugroho A, Min BK, Kim J (2011) Continuous synthesis of high-surface-area aluminum hydroxide methoxide nano- and microparticles in supercritical methanol and their conversion into  $\gamma$ - $\text{Al}_2\text{O}_3$ . *Mater Lett* 65:772–774
- Wijnja H, Schulthess CP (1999) ATR-FTIR and DRIFT spectroscopy of carbonate species at the aged  $\gamma$ - $\text{Al}_2\text{O}_3$ : water interface. *Spectrochim Acta A* 55:861–872
- Wu Sh, Li F, Wang H, Fu L, Zhang B, Li G (2010a) Effects of poly (vinyl alcohol) (PVA) content on preparation of novel thiol-functionalized mesoporous PVA/ $\text{SiO}_2$  composite nanofiber membranes and their application for adsorption of heavy metal ions from aqueous solution. *Polymer* 51:6203–6211
- Wu Sh, Li F, Xu R, Wei Sh, Wang H (2010b) Preparation of poly (vinyl alcohol)/silica composite nanofibers membrane functionalized with mercapto groups by electrospinning. *Mater Lett* 64:1295–1298
- Xiadong X, Qin W, Jian Y, Liangguo Y, Rui F, Guodong C, Bin D, He L (2012) Highly efficient removal of heavy metal ions by amine-functionalized mesoporous  $\text{Fe}_3\text{O}_4$  nanoparticles. *Chem Eng J* 184:132–140



- Yoo YS, Park KY, Jung KY, Cho SB (2009) Preparation of  $\alpha$ -alumina nanoparticles via vapor-phase hydrolysis of  $\text{AlCl}_3$ . *Mater Lett* 63:1844–1846
- Zhang J, Shi F, Lin J, Wei SY, Chen D, Gao JM, Huang Z, Ding XX, Tang C (2008) Nanoparticles assembly of boehmite nanofibers without surfactant. *Mater Res Bull* 43:1709–1715
- Zhou SX, Antonietti M, Niederberger M (2007) Low-temperature synthesis of  $\gamma$ -alumina nanocrystals from aluminum acetylacetonate in non aqueous media. *Small* 3(5):763–767
- Zhou LM, Wang YP, Liu ZR, Huang QW (2009) Characteristics of equilibrium, kinetics studies for adsorption of  $\text{Hg(II)}$ ,  $\text{Cu(II)}$ , and  $\text{Ni(II)}$  ions by thiourea-modified magnetic chitosan microspheres. *J Hazard Mater* 161:995–1002

